中國機械工程學刊第四十五卷第一期第 57~66 頁(民國一百一十三年)
Journal of the Chinese Society of Mechanical Engineers, Vol.45, No.1, pp 57~66 (2024)

Fracture Analysis for Angled Surface, Corner and Edge Cracks in Rails Subjected to Bending Loads

Oğuzhan Demir

Keywords：fracture, stress intensity factors, surface cracks, edge cracks, corner cracks.

ABSTRACT

In this study, three-dimensional stress intensity factor (SIF) solutions for inclined and deflected surface, corner and edge cracks in rails subjected to bending loads are presented. Fracture analyses are performed using FRAC3D, which is part of Fracture and Crack Propagation Analysis System (FCPAS), employing fully unstructured tetrahedral elements along the crack front and in the whole model. The results of the analyses declare how the SIF distributions along the crack front having with different configurations variate with the change of the crack orientations and which crack type is critical in rails. It is observed that increasing the inclination or deflection angle results in a decrease in mode-I SIFs and increases in mode-II and mode-III SIFs. The decrease in mod-I SIF ranges from about 6.3~6.4 MPa$\sqrt{m}$ to about 1.4~1.5 MPa$\sqrt{m}$ with increasing the inclination or deflection angle from 0° to 75° for the edge or surface cracks while it changes from about 4.48 MPa$\sqrt{m}$ to about 0.5 MPa$\sqrt{m}$ for the corner crack under constant design load conditions. It is shown that the distributions and magnitudes of mixed mode SIFs for the edge and the surface cracks are very similar for both crack orientations. The results also show that the corner crack is a less risky damage type compared to the edge and the surface cracks for rails subjected to bending load since the dominant mode-I SIFs obtained for the corner crack are generally much smaller than other cases for both crack orientations.

INTRODUCTION

Cracks are encountered in many structural parts at different locations, due to many reasons such as internal defects (porosity, inclusions) derived from manufacturing processes or different causes such as environmental surroundings, boundary and loading conditions, etc. Cracks in the structure may remain stable up to a certain safe size for many years, or they may suddenly become unstable and propagate up to failure, causing serious accidents, financial losses, and even loss of life in some cases. Therefore, determining and knowing the response of the components including cracks against possible damages is significant in designing structures considering different parameters to ensure safe use of elements i.e., to design structures with damage/tolerance and to determine fail-safe/remaining life assessment. A numerical assessment of damaged structures containing cracks requires an accurate and precise computation of fracture parameters. Most of these cracks appear in the structures as surface, edge or corner cracks and need to be analyzed using three-dimensional approaches. Many fracture phenomena encountered today include mixed mode fracture conditions due to different causes such as the relative orientation of crack surfaces as regards to the loading direction, mixed mode or multi-axial loads, boundary conditions, etc. Thus, for such mixed mode fracture problems, from which the initial crack may be in inclined and/or deflected form or may propagate in such of these forms, three-dimensional modeling capabilities and solutions are needed for a thorough understanding of mechanisms driving mixed mode fracture. It is well known that the accurate and precise calculation of three-dimensional mixed mode stress intensity factors (SIFs), i.e., K_I, K_{II}, and K_{III} along the crack front has a remarkable role on mixed mode fracture analysis.

The research studies performed for the analysis of three-dimensional fracture and crack propagation problems numerically have become popular with the rapid growth of particular tools, techniques or methods after the late of 1960s. Boundary elements method (Ingraffea et al., 1983; Sousa et al., 1989; Wawrzynek et al., 1988), alternating methods (Hartranft and Sih, 1973; Shah and Kobayashi, 1973; Smith et al., 1967; Smith and Alavi, 1971; Thresher and Smith, 1972), line-spring method ((Delale and

Paper Received April, 2023. Revised July, 2023. Accepted August, 2023. Author for Correspondence: Oğuzhan Demir

Associate Professor, Department of Mechanical Engineering, Bilecik Seyh Edebali University, Bilecik, Turkey 11230.

Erdogan, 1981; German et al., 1983; Miyoshi et al., 1986; Parks and White, 1982; Rice and Levy, 1972), virtual crack extension method (Blackburn and Hellen, 1977; Dixon and Pook, 1969; Hellen, 1975; Watwood Jr, 1969), and finite element methods (Barsoum, 1976; Levy et al., 1971; Marcal et al., 1973; Steinmueller, 1974; Tracey, 1974; Zienkiewicz and Cheung, 1967) are some of the employed numerical procedures to analyze such problems. The finite element method is very prevalent among them.

Several simulation software such as FRANC3D (Carter et al., 1995, 2000), ZENCRACK (Hou et al., 2001; ZENCRACK, 1999), ADAPCRACK3D (Schöllmann et al., 2003), BEASY (Curtin et al., 1999; Neves et al., 1997) and FRAC3D (Ayhan and Nied, 1998, 2002) have been developed using such methods for the analysis of three-dimensional fracture mechanics problems. FRANC3D, ZENCRACK and BEASY can promote the most well-known finite element-based codes, namely NASTRAN, ANSYS and ABAQUS. ADAPCRACK3D software works in conjunction with ABAQUS and uses the finite element method. FRAC3D is part of Fracture and Crack Propagation Analysis System (FCPAS) and uses the enriched finite element method for fracture analysis. The enriched finite element method permits accurate and direct computation of fracture parameters with no pre- and post-process interventions and without the need a special mesh structure near the crack front. FRAC3D employs enriched finite elements along the crack tip to compute stress intensity factors (SIFs). Several studies have been successfully carried out by FRAC3D for fracture problems containing interface cracks (Ayhan et al., 2006), mode-I (Ayhan and Nied, 2002; Uslu et al., 2014a, 2014b) and mixed mode cracks (Ayhan, 2004, 2007a, 2007b, 2009; Ayhan and Demir, 2021; Demir, 2021). One of the main reasons for fracture and damage problems faced with today in many practical engineering applications is the exposure of structural parts to mixed mode fracture conditions (Demir et al., 2017, 2018; Yaren et al., 2019). Liu et al. (2020) analyzed the fatigue crack growth behavior of transverse surface cracks in rail steel and thermite weld under in-plane and out-of-plane loading. It was indicated that out-of-plane bending load was more remarkable failure mode than in-plane bending load for thermite weld joints in curve tracks. Lian et al. (2019) investigated the white etching layer (WEL) on rail surfaces, identifying three distinct crack patterns within the WEL and evaluating crack propagation using a finite element model. The study revealed shear mode as the dominant mechanism for crack propagation, with leading cracks showing the highest potential for growth. Ringsberg (2005) studied the surface-breaking cracks in a twin disc test specimen using elastic-plastic finite element calculations and fracture mechanics theory. The study showed that shear crack growth dominates for all crack lengths tested, with the potential for spalling failure in longer cracks.

Bold et al. (1991) investigated the mixed mode crack growth conditions for rolling contact fatigue surface cracks. They showed that the crack growth direction was on the plane of the maximum shear stress rather than perpendicular to the maximum tangential stress as occurs by a conventional fatigue testing. Three-dimensional finite element analyses for wheel-rail system with an initial subsurface crack in the rail were carried out by Fang et al. (2022a, 2022b). The studies examine the mixed fatigue crack growth behavior of rail. It was found that the subsurface fatigue crack propagation of rail was mixed mode II/III and dominant mode was the slip propagation of mode II. Lesiuk et al. (2020) performed mode-I and mixed mode-I/II fatigue crack growth experiments in rail steel to understand the fatigue behavior. They used compact tension specimens (CTS) and finite element method to determine SIFs and discussed the impact of elastic mixity on fatigue crack growth rates and directions. Non-proportional mixed mode-I/II/III behavior in rolling contact fatigue cracks in rails were investigated by Bonniot et al. (2018). Through asymmetric four-point bending tests on rail steel, they assessed crack growth thresholds and kinetics in mixed mode-II/III and successfully predicted crack front paths and growth rates using effective SIFs derived from measured crack face displacements.

It is seen from the literature that numerous studies published in recent years have focused on mixed mode fracture analyses of rails. In various engineering problems encountered today, mixed mode fracture conditions arise due to factors like multi-axial and mixed mode loads, non-perpendicular orientation of crack surfaces concerning uniaxial loading, and diverse boundary conditions. To accurately assess such conditions computationally, a comprehensive understanding of the mechanisms governing mixed mode fracture is essential. This requires knowledge of the mixed mode crack driving forces, i.e., SIFs, under specific loading conditions.

Cracks or fracture problems that may occur in railway axles, rails or train wheels due to many reasons such as environmental factors, manufacturing type, material, or applied loads may become extremely crucial. Crack can remain in the rail until a certain safe size or sometimes with a sudden fracture may cause serious accidents leading to catastrophic failures and even in some cases may cause loss of lives. Indeed, accurate and precise computation of fracture parameters is crucial to prevent damaging situations and ensure the safe functioning of cracked structures. This allows for fail-safe and remaining life assessments, enabling a thorough evaluation of the structural integrity and potential risks associated with the damaged components.

The level of mode mixity ratio directly affects the magnitude and distribution of SIFs along the crack front and influences the characteristics of crack growth surface and the critical fracture load limit required for unstable fracture. Therefore, to evaluate together all the three fundamental fracture modes, i.e., mode-I, mode-II and mode-III, play a significant role in prediction of critical fracture loads, crack growth angle and crack propagation rate histories (Ayhan and Demir, 2019; Demir et al., 2019).

In this study, three-dimensional fracture analyses performed for inclined and deflected surface, corner and edge cracks in rails subjected to bending loads are presented. The mixed mode SIF solutions are obtained using FRAC3D.

PROBLEM DESCRIPTION

In this section, mixed mode fracture cases containing different crack configurations and orientations are depicted with regard to geometry and loading details. A UIC60 rail profile is used for three-dimensional fracture analyses.

A uniform bending moment (ΔM = 37.62 kNm) is applied to the end of the rail section and the other end is fixed (Figure 1-a). The rail section length is 200 mm and the initial crack dimensions, crack depth (a) and a half crack length (c) are a =c= 3 mm for all the considered cases. In Fig. 1, the loading details and considered crack configurations are given. The edge, corner and surface cracks with different deflection and inclination angles ranging from 0° to 75° in steps of 15° are analyzed. The initial cracks are located on the half section length. In the case of an inclined crack, the crack plane is rotated with respect to the "x" axis by "α" for which axis representations are given in Fig. 1-b for each crack configurations. In the case of a deflected crack, the crack plane is rotated with respect to the "y" axis by "θ" (Fig. 1-b). The inclination and deflection angles are measured from a plane parallel to the x–y plane. To clarify the difference between the inclination and deflection angles, representative crack configurations for a 45° crack angle are depicted in Fig. 1-b.

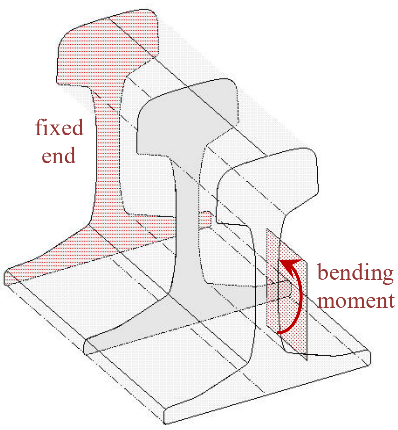

(a)

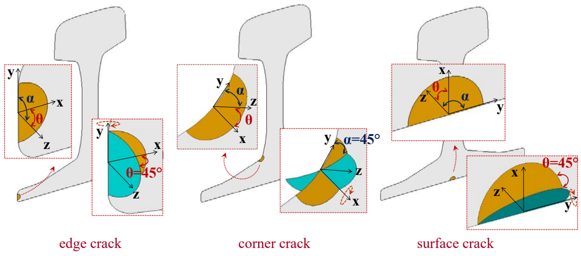

(b)

Fig. 1. (a) The loading details and (b) crack configurations.

NUMERICAL RESULTS

The finite element models for all fracture analyses performed in the study are obtained using ANSYS™ (ANSYS, 2009). The files related with the finite element model such as element and node lists of the crack front and of the whole model, load, displacement lists are converted for importing these data into FRAC3D solver (Ayhan and Nied, 1998; 2002) where the SIF distributions along the crack front are computed by employing 3-D tetrahedral enriched elements. A set of mesh sensitivity analyses are performed to obtain optimum mesh structures, and accurate and precise analysis results. It is ascertained from the results of detailed sensitivity analyses, the ratio of the half crack length (c) or the crack depth (*a*) (whichever is smaller) to the crack tip element size (S_{tip}), in vertical directions to the crack front can be taken as *(a or c)/*S_{tip}= 100.

The material properties used in all analyses are Young's modulus E=210 GPa and Poisson's ratio ν=0.3. The general and close-up views of the crack region of the finite element model containing corner crack (α=θ=0°) are given in Figure 2. As mentioned above, 3-D enriched crack tip finite elements are employed for computation of 3-D mixed mode SIFs, K_I, K_{II}, and K_{III} along the crack front. It is seen from the figure that enriched crack tip finite elements are the orange-colored elements that surround the crack front and transition finite elements (blue-colored) are located between the enriched and the regular finite elements.

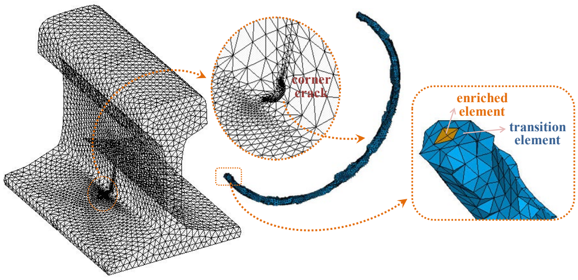

Fig. 2. Finite element model of the crack region for corner crack (α= θ=0°).

The finite element model given in Fig. 2 is meshed with fully 10-noded tetrahedral elements. The model includes 401 nodes and 3658 enriched elements along the crack front, and a total of 172,075 nodes and 118,341 elements in the whole model. Figure 3 shows the von Mises stress distributions around the crack regions obtained for some crack configurations. It is seen that, as expected, high stress concentrations exist around the crack regions.

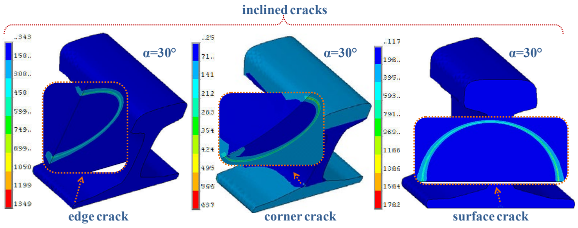

(a)

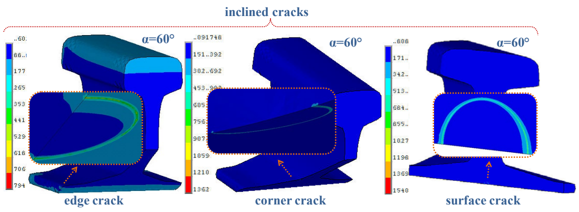

(b)

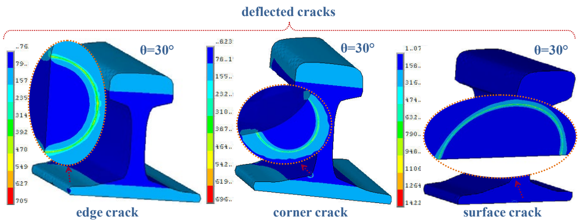

(c)

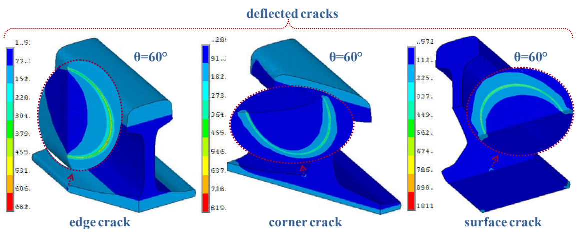

(d)

Fig. 3. von Mises stress distributions around the crack regions obtained for the models, (a) α=30°, (b) α=60°, (c) θ=30°, (d) θ=60°.

In Figure 4, distributions of mixed mode SIFs along the crack front obtained for an edge crack with different inclination angles are given. It should be noted that when tetrahedral elements are used along the crack front, an oscillatory SIF variation is occurred due to the nonuniform and irregular sequence of finite elements. Therefore, the distributions of the resulting SIFs from fracture analyses performed in this study are smoothed.

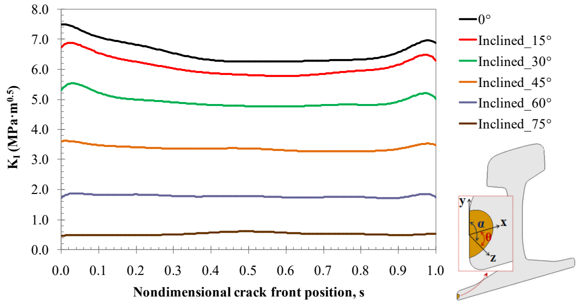

(a)

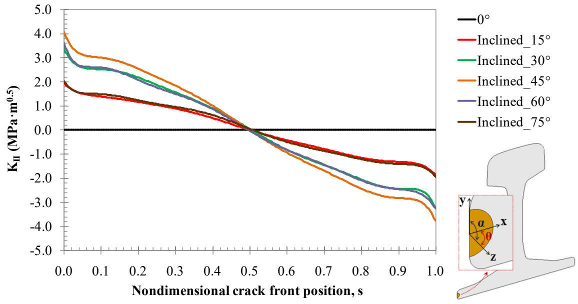

(b)

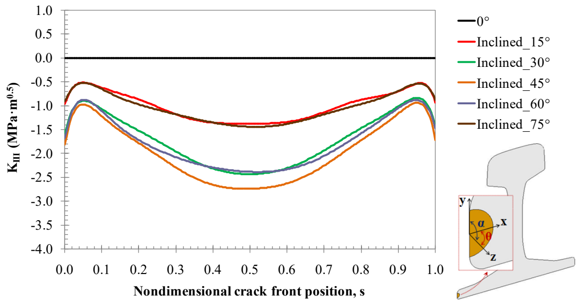

(c)

Fig. 4. Mixed mode SIFs along the crack front obtained for an edge crack with different inclination angles (a) K_I, (b) K_{II}, (c) K_{III} distributions.

As can be seen from Fig.4(a) that as the inclination (α) angle increases the K_I SIFs decrease and the maximum value is attained for the non-inclined case, i.e., under pure mode-I loading (α=0°). It should be noted based on the literature (Bažant & Estenssoro, 1979; Benthem, 1977; Pook et al., 2017) that at the zone in which the crack front crosses the free-surface, the stress and strain singularities are different than the inverse square root singularity characteristic ($r^{1/2}$) and are influenced by the Poisson’s ratio and the intersection angle. Since mixed mode SIFs can be computed correctly near the free-surface, a particular transaction is not executed to obtain the actual SIF values in the close vicinity of the free surface for all analyses carried out in this study. It is seen in Fig.4b that, the K_{II} SIFs increase with increasing inclination angle until α=45° and then decrease. The K_{II} SIF along the whole crack front is zero at α=0° and its distribution is linear and anti-symmetric and since it is on the symmetry surface, the value is zero at the crack's deepest point for all non-zero inclination angles. The highest values are obtained for mode-II at α=45° (the plane with the maximum shear stress). The K_{II} SIFs are almost equal for α=15°-75° and α=30°-60° since these angles are the complementary inclination angles. Similar to the behavior of K_{II} SIF, K_{III} SIF is zero at α=0°, as this loading condition depicts a pure mode-I loading case, and increases in magnitude until α=45° in which takes its highest value. The K_{III} SIFs are almost equal for the complementary angles. Symmetrical distribution along the crack front is observed for mode-III SIFs and their values are highest at the crack's deepest point for all non-zero inclination angles. Figure 5 shows the distributions of mixed mode SIFs along the crack front obtained for a corner crack with different inclination angles. It is deduced from Fig. 5 that as the inclination (α) angle increases the K_I SIFs decrease and the maximum value is attained for α=0° while the K_{II} and K_{III} SIFs are zero at this inclination angle. It is also observed that mode-I SIF becomes negative partially at the close vicinity of the free-surface for α=75°, reflecting crack surface contact.

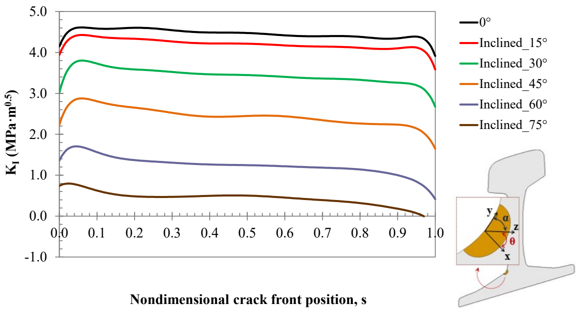

(a)

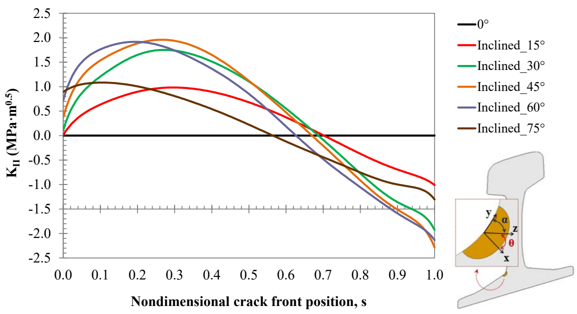

(b)

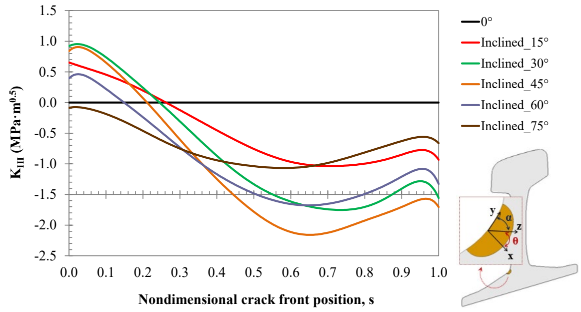

(c)

Fig. 5. Mixed mode SIFs along the crack front obtained for a corner crack with different inclination angles (a) K_I, (b) K_{II}, (c) K_{III} distributions.

Similar to the behavior of the edge crack configuration, K_{II} and K_{III} SIFs increase until α=45° and then decrease for α=60° and α=75° as the effective shear stresses causing the mode-II and mode-III SIFs also decrease. The mixed mode SIF distributions along the crack front obtained for a corner crack with different inclination angles are presented in Figure 6. As seen from the graphs, distributions of the mixed mode SIFs behave similar to those in Fig. 4, i.e., the edge and the surface crack with the same size exhibit similar behaviors in terms of obtained SIF variations under the same loading situations. Fracture analyses are also performed for the cracks with different deflection angles as is the case with the cracks containing different inclination angles and the resulting SIF distributions are discussed below.

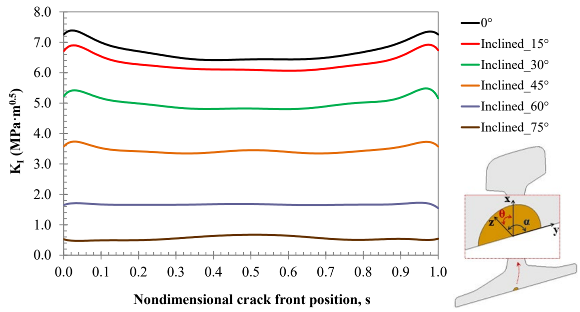

(a)

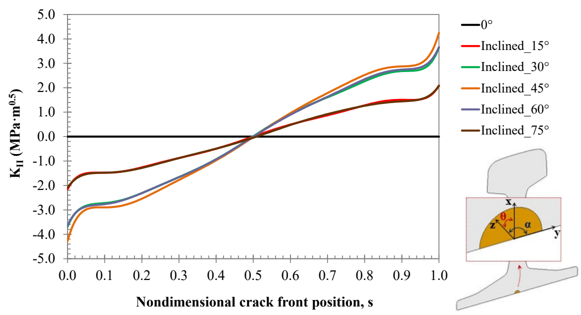

(b)

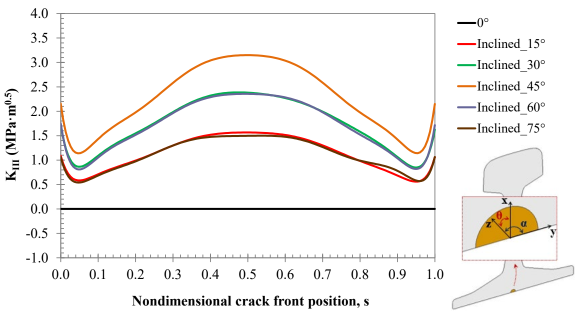

(c)

Fig. 6. Mixed mode SIFs along the crack front obtained for a surface crack with different inclination angles (a) K_I, (b) K_{II}, (c) K_{III} distributions.

Figure 7 shows variations of mixed mode SIFs, K_I, K_{II} and K_{III} along the crack front for an edge crack with different deflection angles. As is seen from Fig.7a that as the deflection (θ) angle increases the K_I SIFs decrease and the value is maximum for the non-deflected case, i.e., pure mode-I (θ=0°) loading condition. The K_{II} and K_{III} SIFs increase with increasing deflection angle until θ=45°, then decrease and their values along the whole crack front are zero at α=0° (Fig. 7b-c). Maximum value for mode-II SIF is obtained at the deepest point for all non-zero deflection angles. The K_{III} SIF distribution is linear and anti-symmetric and its value is zero at the deepest point for all non-zero deflection angles due to the symmetry surface.

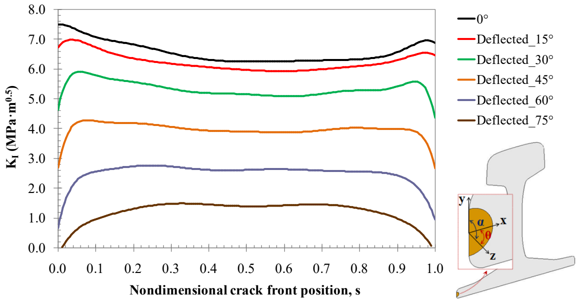

(a)

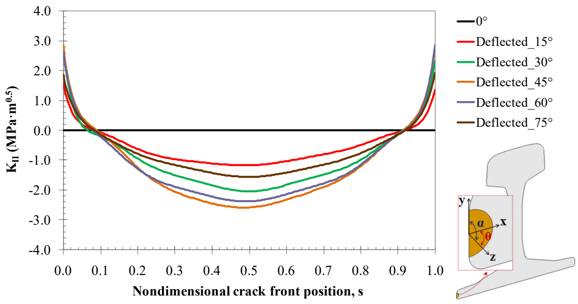

(b)

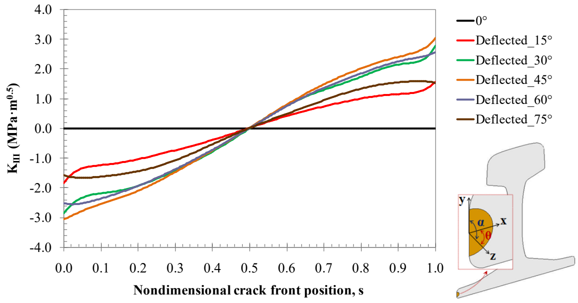

(c)

Fig. 7. Mixed mode SIFs along the crack front obtained for an edge crack with different deflection angles (a) K_I, (b) K_{II}, (c) K_{III} distributions.

The mixed mode SIF distributions obtained for a corner crack with different deflection angles are plotted in Figure 8. Similar to the behavior of edge crack configuration, as the deflection (θ) angle increases the K_I SIF decreases and its value is maximum for θ=0° while the K_{II} and K_{III} SIFs are zero at this angle. Also, the K_{II} and K_{III} SIFs increase until α=45° and then decrease for α=60° and α=75°.

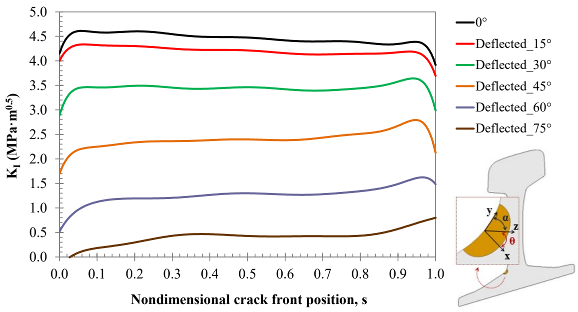

(a)

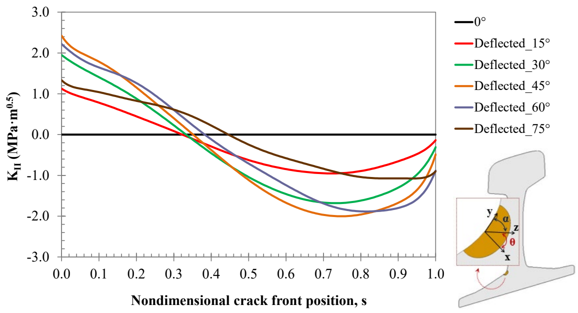

(b)

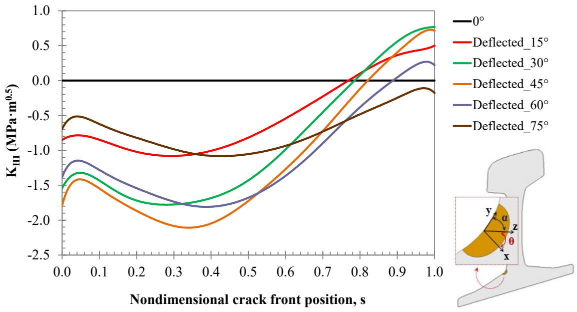

(c)

Fig. 8. Mixed mode SIFs along the crack front obtained for a corner crack with different deflection angles (a) K_I, (b) K_{II}, (c) K_{III} distributions.

Finally, the computed SIFs for a surface crack with different deflection angles are shown in Figure 9.

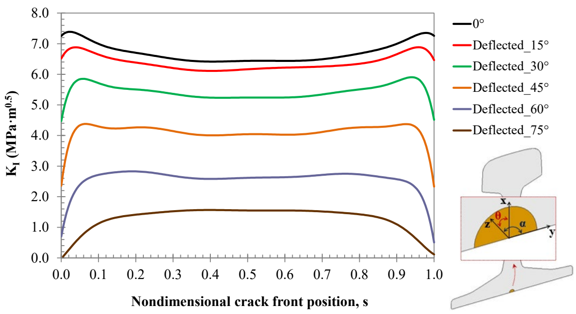

(a)

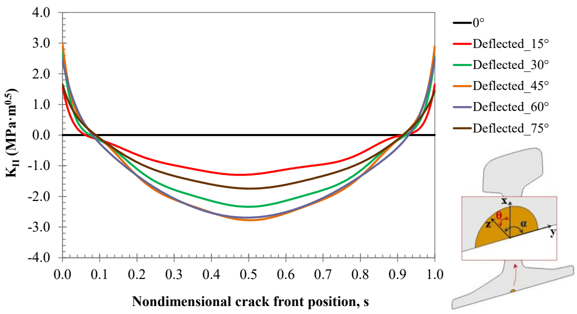

(b)

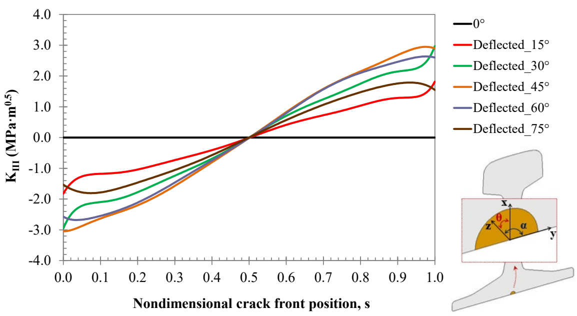

(c)

Fig. 9. Mixed mode SIFs along the crack front obtained for a surface crack with different deflection angles (a) K_I, (b) K_{II}, (c) K_{III} distributions.

It is deduced from the graphs that variations of mixed mode SIFs along the crack front are very similar to those in Fig. 7, as is the case with the inclined crack configurations.

CONCLUSIONS

This paper provides mixed-mode SIF solutions for deflected and inclined surface, corner and edge cracks in rails subjected to bending loads. Three-dimensional fracture analyses were performed employing enriched finite elements along the crack front using FRAC3D, which is a general-purpose standalone fracture analysis program. The following conclusions could be made:

(i) For all crack configurations, the K_I SIFs decrease with increasing the deflection or inclination angle.

(ii) For all crack configurations, the K_{II} and KIII SIFs increase until the deflection or inclination angle of 45 and then decrease with increasing the deflection or inclination angle.

(iii) The distributions and magnitudes of mixed mode SIFs along the crack front for the edge and the surface cracks are almost identical for both crack orientations.

(iv) The K_I SIF values computed for the corner crack are generally much smaller than the edge and the surface cracks for both crack orientations. Thus, the corner crack is a less risky damage type compared to other cases for rails under bending load, when considered that the dominant mode-I SIFs obtained for the corner crack are the smallest.

As a future work, fracture and fatigue crack growth experiments and experimental applications using strain-gages are also being planned to validate the results presented in the study.

Data Availability Statement

Some or all data, models, or code that support the findings of this study are available from the corresponding author upon reasonable request.

Compliance with Ethical Standards

Funding: The author did not receive support from any organization for the submitted work.

Conflict of interest: The author declares that he has no conflict of interests.

ACKNOWLEDGEMENT

The support by Dr. Ali O. Ayhan is gratefully acknowledged for providing FCPAS software.

REFERENCES

Aurell, J. and Edlund, S., "The Influence of Steered Axles on the Dynamic Stability of Heavy Vehicles," *SAE paper* No. 892498 (1989).

Bernard, J.E., Vanderploeg, M.J., and Shannan, J.E, "Linear Analysis of a Vehicle with Four-Wheel Steering," *SAE paper* No. 880643 (1988).

Furleigh, D.D., Vanderploeg, M.J., and Oh, C.Y., "Multiple Steered Axles for Reducing the Rollover Risks of Heavy Articulated Trucks," *SAE paper* No.881866 (1988).

Kang, X, Rakheja, S. and Stiharu, I., "Effects of Tank Shape on the Roll Dynamic Response of a Partly Filled Tank Vehicle," *Veh. Sys. Dyn.*, Vol.35, No.2, pp.75-102 (2000).

LeBlane, P.A., El-Gindy, M. and Woodrooffe, J.H.F., "Self-steering axles:Theory and Practice," *SAE paper* No.891633 (1989).

Rakheja, S., "Roll Plane Analysis of Articulated Tank Vehicles During Steady Turning," *Veh. Sys. Dyn.*, Vol. 17, pp.81-104 (1988).

Ranganathan, R., Rakheja, S., Sankar, S., "Steady Turning Stability of Partially Filled Tank Vehicles With Arbitrary Tank Geometry," *J. Dyn. Sys. Measur. Contr.*, Vol. 111, No. 3,pp. 481-489 (1989).

Ranganathan, R., "Influence of Liquid Load Shift on the Dynamic Response of Articulated Tank Vehicles," *Veh. Sys. Dyn.*, Vol.19, pp.177-200 (1990).

Sano, S., Furukawa, Y. and Shiraishi, S., "Four-Wheel Steering System with Rear Wheel Steer Angle Controlled as a Function of Steering Wheel Angle," *SAE Trans. paper* 860625 (1986).

Wang, J.Y., *Theory of Ground Vehicles*, John Wiely, New York (1993).

Wu, D-H, "A Theoretic Study for Yaw/Roll Motions of Multiple Steering Articulated Vehicle," *Pro. I. Mech. Eng. Part D.,* Vol. 215, pp.1257-1265 (2001).

Ayhan, A. O., "Mixed mode stress intensity factors for deflected and inclined surface cracks in finite-thickness plates," *Engineering Fracture Mechanics*, Vol.71, No.7–8, pp.1059–1079 (2004).

Ayhan, A. O. "Mixed mode stress intensity factors for deflected and inclined corner cracks in finite-thickness plates," *International Journal of Fatigue*, Vol.29, No.2, pp.305–317 (2007a).

Ayhan, A. O., "Stress intensity factors for three-dimensional cracks in functionally graded materials using enriched finite elements," *International Journal of Solids and Structures*, Vol.44, No.25–26, pp.8579–8599 (2007b).

Ayhan, A. O., "Three-dimensional mixed-mode stress intensity factors for cracks in functionally graded materials using enriched finite elements," *International Journal of Solids and Structures*, Vol.46, No.3–4, pp.796–810 (2009).

Ayhan, A. O., and Demir, O., "A novel test system for mixed mode-I/II/III fracture tests-Part 1: Modeling and numerical analyses," *Engineering Fracture Mechanics*, Vol.218, *paper* No.106597 (2019).

Ayhan, A. O., and Demir, O., "Computational modeling of three-dimensional mixed mode-I/II/III fatigue crack growth problems and experiments," *Computers & Structures*, Vol.243, *paper* No.106399 (2021).

Ayhan, A. O., Kaya, A. C., and Nied, H. F., "Analysis of three-dimensional interface cracks using enriched finite elements," *International Journal of Fracture*, Vol.142, No.3–4, pp.255–276 (2006).

Ayhan, A. O., and Nied, H. F., "FRAC3D-Finite element based software for 3-D and generalized plane strain fracture analysis," *Semiconductor Research Corporation (SRC) Technical Report* (1998).

Ayhan, A. O., and Nied, H. F., "Stress intensity factors for three-dimensional surface cracks using enriched finite elements," *International Journal for Numerical Methods in Engineering*, Vol.54, No.6, pp.899–921 (2002).

ANSYS, Theory manual version 12.0, *Ansys Inc*. (2009).

Barsoum, R. S., "On the use of isoparametric finite elements in linear fracture mechanics," *International Journal for Numerical Methods in Engineering*, Vol.10, No.1, pp.25–37 (1976).

Bažant, Z. P., and Estenssoro, L. F., "Surface singularity and crack propagation," *International Journal of Solids and Structures*, Vol.15, No.5, pp.405–426 (1979).

Benthem, J., "State of stress at the vertex of a quarter-infinite crack in a half-space," *International Journal of Solids and Structures*, Vol.13, No.5, pp.479–492 (1977).

Blackburn, W. S., and Hellen, T. K., "Calculation of stress intensity factors in three dimensions by finite element methods," *International Journal for Numerical Methods in Engineering*, Vol.11, No.2, pp.211–229 (1977).

Bold, P. E., Brown, M. W., and Allen, R. J., "Shear mode crack growth and rolling contact fatigue", *Wear,* Vol.144, No.1-2, pp.307-317 (1991).

Bonniot, T., Doquet, V., and Mai, S. H., "Mixed mode II and III fatigue crack growth in a rail steel", *International Journal of Fatigue*, Vol.115, pp.42-52 (2018).

Carter, B. J., Ingraffea, A. R., and Bittencourt, T. N., "Topology-controlled modeling of linear and nonlinear 3D crack propagation in geo-materials," In G. Baker and B. L. Karihaloo (Eds.), *Fracture of Brittle Disordered Materials: Concrete, Rock and Ceramics* (First edit, pp. 301–318). E&FN Spon Publishers Brisbane, Australia (1995).

Carter, B. J., Wawrzynek, P. A., and Ingraffea, A. R., "Automated 3-D crack growth simulation," *International Journal for Numerical Methods in Engineering*, Vol.47, No.1–3, pp.229–253 (2000).

Curtin, T. J., Adey, R. A., Baynham, J. M. W., and Marais, P., "Fatigue Crack Growth Simulation for Complex Three-Dimensional Geometry and Loading," *Nasa Conference Publication*, pp.657–666 (1999).

Delale, F., and Erdogan, F., "Line-spring model for surface cracks in a Reissner plate," *International Journal of Engineering Science*, Vol.19, No.10, pp.1331–1340 (1981).

Demir, O., "Three-dimensional modeling of non-planar fatigue crack growth in spur gear tooth using tetrahedral finite elements," *Engineering Fracture Mechanics*, Vol.252, *paper* No.107857 (2021).

Demir, O., Ayhan, A. O., and Iriç, S., "A new specimen for mixed mode-I/II fracture tests: Modeling, experiments and criteria development," *Engineering Fracture Mechanics*, Vol.178, pp.457–476 (2017).

Demir, O., Ayhan, A. O., and Iriç, S., "A novel test system for mixed mode-I/II/III fracture tests-Part 2: Experiments and criterion development," *Engineering Fracture Mechanics*, Vol.220, *paper* No.106671 (2019).

Demir, O., Ayhan, A. O., Sedat, I., and Lekesiz, H., "Evaluation of mixed mode-I/II criteria for fatigue crack propagation using experiments and modeling," *Chinese Journal of Aeronautics*, Vol.31, No.7, pp.1525–1534 (2018).

Dixon, J. R., and Pook, L. P., "Stress intensity factors calculated generally by the finite element technique," *Nature*, Vol.224, No.5215, pp.166–167 (1969).

Fang, X.Y., Zhang, H. N., Ma, D. W., Wu, Z. J., and Huang, W., "Influence of welding residual stress on subsurface fatigue crack propagation of rail", *Engineering Fracture Mechanics*, Vol.271, *paper* No.108642 (2022a).

Fang, X. Y., Zhang, H. N., Ma, D. W., "Influence of initial crack on fatigue crack propagation with mixed mode in U71Mn rail subsurface", *Engineering Failure Analysis*, Vol.136, *paper* No.106220 (2022b)

German, M. D., Kumar, V., and De Lorenzi, H. G., "Analysis of surface cracks in plates and shells using the line-spring model and ADINA," *Computers & Structures*, Vol.17, No.5–6, pp.881–890 (1983).

Hartranft, R. J., and Sih, G. C., "Alternating method applied to edge and surface crack problems," In G. C. Sih (Ed.), *Methods of analysis and solutions of crack problems,* pp.179–238, Springer (1973).

Hellen, T. K., "On the method of virtual crack extensions," *International Journal for Numerical Methods in Engineering*, Vol.9, No.1, pp.187–207 (1975).

Hou, J., Goldstraw, M., Maan, S., and Knop, M., "*An evaluation of 3D crack growth using ZENCRACK*," *Technical Report* pp.1-27 (2001).

Ingraffea, A. R., Blandford, G. E., and Liggett, J. A., "Automatic modelling of mixed-mode fatigue and quasi-static crack propagation using the boundary element method," *Fracture Mechanics: Fourteenth Symposium—Volume I: Theory and Analysis* (1983).

Lesiuk, G., Smolnicki, M., Mech, R., Zięty, A., Fragassa, C., "Analysis of fatigue crack growth under mixed mode (I+ II) loading conditions in rail steel using CTS specimen", *Engineering Failure Analysis*, Vol.109, *paper* No.104354 (2020).

Levy, N., Marcal, P. V, and Rice, J. R., "Progress in three-dimensional elastic-plastic stress analysis for fracture mechanics," *Nuclear Engineering and Design*, Vol.17, No.1, pp.64–75 (1971).

Lian, Q., Deng, G., Al-Juboori, A., Li, H., Liu, Z., Wang, X., Zhu, H., "Crack propagation behavior in white etching layer on rail steel surface", *Engineering Failure Analysis*, Vol.104, pp.816-829 (2019).

Liu, Y., Tsang, K. S., Hoh, H. J., Shi, X., and Pang, H. L., "Structural fatigue investigation of transverse surface crack growth in rail steels and thermite welds subjected to in-plane and out-of-plane loading", *Engineering Structures*, Vol. 204, *paper* No.110076 (2020).

Marcal, P. V, Stuart, P. M., and Bettes, R. S., "Elastic-plastic behavior of a longitudinal semi-elliptic crack in a thick pressure vessel," (No. HSSTP-TR-28) Brown Univ. (1973).

Miyoshi, T., Shiratori, M., and Yoshida, Y., "Analysis of J-integral and crack growth for surface cracks by line-spring method," *J. Press. Vess. Technol.*, Vol.108, pp.305–311 (1986).

Neves, A. C., Adey, R. A., Baynham, J. M. W., and Niku, S. M., "Automatic 3D crack growth using BEASY," *WIT Transactions on Modelling and Simulation*, Vol.19, pp.819–827 (1997).

Parks, D. M., and White, C. S., “Elastic-plastic line-spring finite elements for surface-cracked plates and shells,” *J. Press. Vess. Technol.*, Vol.104, pp.287–292 (1982).

Pook, L. P., Berto, F., and Campagnolo, A., “State of the art of corner point singularities under in-plane and out-of-plane loading,” *Engineering Fracture Mechanics*, Vol.174, pp.2–9 (2017).

Rice, J. R., and Levy, N., “The part-through surface crack in an elastic plate,” *J. Appl. Mech.*, Vol.39, No.1, pp.185–194 (1972).

Ringsberg, J. W., “Shear mode growth of short surface-breaking RCF cracks”, *Wear*, Vol.258, No.7-8, pp.955-963 (2005).

Schöllmann, M., Fulland, M., and Richard, H. A., “Development of a new software for adaptive crack growth simulations in 3D structures,” *Engineering Fracture Mechanics*, Vol.70, No.2, 249–268 (2003).

Shah, R. C., and Kobayashi, A. S., “Stress intensity factors for an elliptical crack approaching the surface of a semi-infinite solid,” *International Journal of Fracture*, Vol.9, No.2, pp.133–146 (1973).

Smith, F. W., and Alavi, M. J., “Stress intensity factors for a penny shaped crack in a half space,” *Engineering Fracture Mechanics*, Vol.3, No.3, pp.241–254 (1971).

Smith, F. W., Emery, A. F., and Kobayashi, A. S., “Stress intensity factors for semicircular cracks: Part 2—Semi-infinite solid,” *J. Appl. Mech.*, Vol.34, pp.947–952 (1967).

Sousa, J. L., Martha, L. F., Wawrzynek, P. A., and Ingraffea, A. R., “Simulation of non-planar crack propagation in three-dimensional structures in concrete and rock,” *Fracture of Concrete and Rock: Recent Developments*, pp.254–264 (1989).

Steinmueller, G., “Restrictions in the application of automatic mesh generation schemes by ‘isoparametric’ co-ordinates,” *International Journal for Numerical Methods in Engineering*, Vol.8, No.2, 289–294 (1974).

Thresher, R. W., and Smith, F. W. “Stress-intensity factors for a surface crack in a finite solid,” *J. Appl. Mech.*, Vol.39, No.1, pp.195–200 (1972).

Tracey, D. M., “Finite elements for three-dimensional elastic crack analysis,” *Nuclear Engineering and Design*, Vol.26, No.2, pp.282–290 (1974).

Uslu, M., Demir, O., and Ayhan, A. O., “Surface cracks in finite thickness plates under thermal and displacement-controlled loads-Part 1: Stress intensity factors,” *Engineering Fracture Mechanics*, Vol.115, pp.284–295 (2014a).

Uslu, M., Demir, O., and Ayhan, A. O., “Surface cracks in finite thickness plates under thermal and displacement-controlled loads-Part 2: Crack propagation,” *Engineering Fracture Mechanics*, Vol.115, pp.255–269 (2014b).

Watwood Jr, V. B., “The finite element method for prediction of crack behavior,” *Nuclear Engineering and Design*, Vol.11, No.2, pp.323–332 (1969).

Wawrzynek, P. A., Martha, L. F., and Ingraffea, A. R., “A computational environment for the simulation of fracture processes in three dimensions,” *Analytical, Numerical and Experimental Aspects of Three Dimensional Fracture Processes. ASME AMD*, Vol.91, pp.321–327 (1988).

Yaren, M. F., Demir, O., Ayhan, A. O., and Iriç, S., “Three-dimensional mode-I/III fatigue crack propagation: Computational modeling and experiments,” *International Journal of Fatigue*, Vol.121, pp.124–134 (2019).

ZENCRACK, user manual, Issue 6, Zentech Inc. (1999).

Zienkiewicz, O. C., and Cheung, Y. K., “The finite element method in structural and continuum mechanics,” McGraw-Hill (1967).